Crystallographic Analysis of Substrate Binding and Catalysis in Dihydrolipoyl Transacetylase (E2p)[†,‡]

Andrea Mattevi, Galya Obmolova, Kor H. Kalk, Alex Teplyakov,[§] and Wim G. J. Hol[*]

BIOSON Research Institute, University of Groningen, Nijenborgh 4, 9747 AG Groningen, The Netherlands

Received September 21, 1992; Revised Manuscript Received January 25, 1993

ABSTRACT: The catalytic domain of dihydrolipoyl transacetylase (E2pCD) forms the core of the pyruvate dehydrogenase multienzyme complex and catalyzes the acetyltransferase reaction using acetylCoA as acetyl donor and dihydrolipoamide ($Lip(SH)_2$) as acceptor. The crystal structures of six complexes and derivatives of *Azotobacter vinelandii* E2pCD were solved. The binary complexes of the enzyme with CoA and $Lip(SH)_2$ were determined at 2.6- and 3.0-Å resolutions, respectively. The two substrates are found in an extended conformation at the two opposite entrances of the 30 Å long channel which runs at the interface between two 3-fold-related subunits and forms the catalytic center. The reactive thiol groups of both substrates are within hydrogen-bond distance from the side chain of His 610. This fact supports the indication, derived from the similarity with chloramphenicol acetyl transferase, that the histidine side chain acts as general-base catalyst in the deprotonation of the reactive thiol of CoA. The conformation of Asn 614 appears to be dependent on the protonation state of the active site histidine, whose function as base catalyst is modulated in this way. Studies on E2pCD soaked in a high concentration of dithionite lead to the structure of the binary complex between E2pCD and hydrogen sulfite solved at 2.3-Å resolution. It appears that the anion is bound in the middle of the catalytic center and is therefore capable of hosting and stabilizing a negative charge, which is of special interest since the reaction catalyzed by E2pCD is thought to proceed via a negatively charged tetrahedral intermediate. The structure of the binary complex between E2pCD and hydrogen sulfite suggests that transition-state stabilization can be provided by a direct hydrogen bond between the side chain of Ser 558 and the oxy anion of the putative intermediate. In the binary complex with CoA, the hydroxyl group of Ser 558 is hydrogen bonded to the nitrogen atom of one of the two peptide-like units of the substrate. Thus, CoA itself is involved in keeping the Ser hydroxyl group in the proper position for transition-state stabilization. Quite unexpectedly, the structure at 2.6-Å resolution of a ternary complex in which CoA and $Lip(SH)_2$ are simultaneously bound to E2pCD reveals that CoA has an alternative, nonproductive binding mode. In this abortive ternary complex, CoA adopts a helical conformation with two intramolecular hydrogen bonds and the reactive sulfur of the pantetheine arm positioned 12 Å away from the active site residues involved in the transferase reaction. The same CoA conformation is observed in the ternary complex with CoA and dithiothreitol. The latter behaves like a substrate analogue which binds in the $Lip(SH)_2$ binding pocket. The strict conservation of the active site residues among the transacylases forming the core of the branched-chain oxo acid dehydrogenase and the oxoglutarate dehydrogenase multienzyme complexes indicates that these enzymes all share the same catalytic mechanism as dihydrolipoyl transacetylase. The investigation of the three-dimensional structure of E2pCD combined with the analysis of the amino acid sequences suggests that the nature and size of only a few side chains might be the major determinants for tuning substrate specificity among the various transacylases.

The oxo acid dehydrogenases form a family of multienzyme complexes (Reed, 1974) which comprises the pyruvate dehydrogenase, the oxoglutarate dehydrogenase, and the branched-chain oxo acid dehydrogenase. The molecular weights of these systems are usually in the range of 3–10 million. They typically consist of multiple copies of at least three enzymes which, by concerting their activities, catalyze the decarboxylation of the 2-oxo acid with the formation of CO_2, acylCoA, and NADH. In all cases, the structural inner core of the complex is formed by the acyltransferase protein (E2) which provides the binding sites for the decarboxylase (E1) and the dehydrogenase (E3) components. Although the size and the composition of the core vary depending on the type of organism (Perham, 1991), in Gram-negative bacteria it always consists of 24 E2 subunits arranged in an oligomeric structure having octahedral 432 symmetry (Oliver & Reed, 1982).

E2 is a modular protein (Perham, 1991) consisting of three types of domains: (i) at the N-terminus one or more lipoyl domains, each carrying a molecule of lipoic acid covalently bound to a lysine side chain; (ii) the E1/E3 binding domain is necessary for the association of the peripheral components of the complex; and (iii) at the C-terminus, the large catalytic domain of 250 residues catalyzes the transferase reaction, $CoA + LipSHS\text{-}acyl \rightarrow acylCoA + Lip(SH)_2$.[1] The catalytic domain is the part of the protein which forms the core of the complex. The domains are connected to each other by short (20–40 residues), flexible segments which are essential for the proper functioning of the complex (Guest et al., 1989; Perham, 1991; Reed & Hackert, 1990). By means of these

[†] This research was supported by the Netherlands Foundation for Chemical Research (SON) with financial aid from the Netherlands Organization for Scientific Research (NWO).

[‡] Protein Data Bank information is as follows: 1EAA, dihydrolipoyl transacetylase native structure; 1EAB, ternary complex with CoA and lipoamide; 1EAC, ternary complex with CoA and DTT; 1EAD, binary complex with CoA; 1EAE, binary complex with lipoamide; 1EAF, binary complex with SO_2OH^-.

[*] Address correspondence and reprint requests to this author at the Department of Biological Structure, SM-20, School of Medicine, University of Washington, Seattle, WA 98195.

[§] EMBL Outstation, 2000 Hamburg 52, FRG.

0006-2960/93/0432-3887$04.00/0

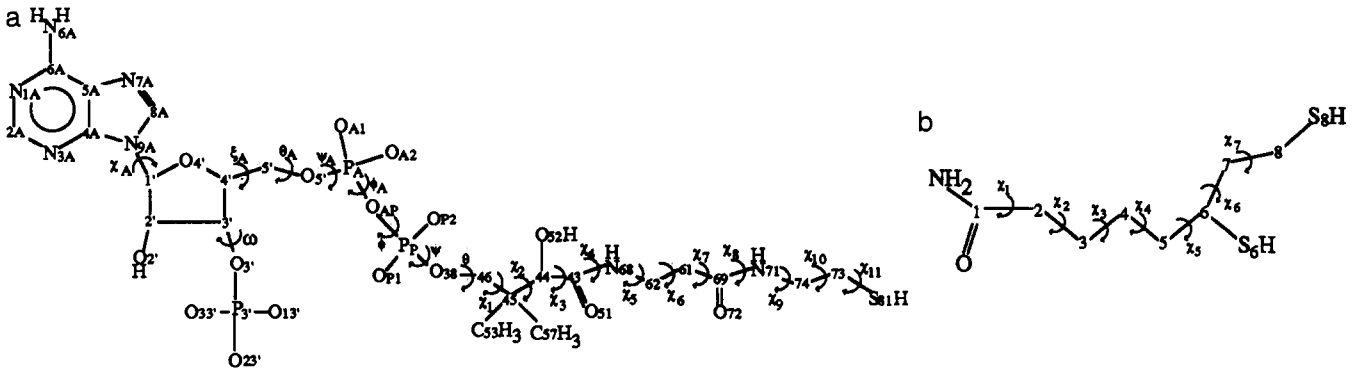

FIGURE 1: Schematic representation of (a) CoA and (b) dihydrolipoamide. The nomenclature adopted for the pantetheine of CoA is identical to that used by Remington et al. (1982). The values of the CoA torsion angles in the IN and OUT conformations are given in Table II.

mobile segments, the lipoyl domains, anchored to the catalytic core, can act as flexible arms, allowing the covalently linked lipoyl group to visit the catalytic sites of the three enzymes whose activities are coupled in this way.

Unlike E3, the E2 and E1 components are specific for each member of the oxo acid dehydrogenase family. Thus, pyruvate decarboxylase (E1p) and dihydrolipoyl transacetylase (E2p) are peculiar to pyruvate dehydrogenase, whereas in oxoglutarate dehydrogenase the analogous enzymes are 2-oxoglutarate decarboxylase (E1o) and dihydrolipoyl transsuccinylase (E2o), respectively. Also, the branched-chain oxo acid dehydrogenase contains specific E1b and E2b components.

The pyruvate dehydrogenase from *Azotobacter vinelandii* is well characterized (Hanemaaijer et al., 1988). The crystal structures of its E3 component (Mattevi et al., 1991) as well as of the catalytic domain (E2pCD) of its E2p component were solved (Mattevi et al., 1992a,b). Particularly, the latter structure determination revealed the inner core of the complex, which is constructed by eight identical trimers each stabilized by a large number of intermolecular contacts. The assembly of the eight trimers gives rise to a remarkable hollow cube with edges of 125 Å. Every individual catalytic domain subunit includes a globular domain, which is topologically identical to chloramphenicol acetyl tranferase (CAT). This agrees with the prediction of Guest (1987) on the basis of a mere 17% sequence homology between the two proteins.

Structural and biochemical investigations (Leslie, 1990; Lewendon et al., 1990) have indicated that the active site of CAT is formed by a channel which traverses the trimer at the interface between two 3-fold-related subunits with the two opposite entrances forming the CoA and chloramphenicol binding sites, respectively. Positioned in the middle of this channel is the side chain of His 195. This residue is essential for catalysis, acting as the general base required for abstracting a proton from the substrate. The structural comparison suggests that the general features of the mechanism proposed for CAT should also be valid for E2pCD, since the regions with the highest similarity between the two enzymes correspond to the CoA binding site and the catalytic center (Mattevi et al., 1992a). Furthermore, His 195 of CAT finds an exact counterpart in His 610 of *A. vinelandii* E2pCD. The catalytic function of the latter side chain is confirmed by mutagenesis experiments on the *Escherichia coli* (Russell & Guest, 1990) and *A. vinelandii* (A. H. Westphal, and A. de Kok, manuscript in preparation) enzymes. However, in the yeast E2p the replacement of the active site histidine with alanine does not cause any change in the enzyme activity (Niu et al., 1990). With the aim of obtaining more insight into substrate binding and catalysis of E2p, we have carried out several crystallographic binding studies by soaking the crystals with the substrates CoA and Lip(SH_2) (Figure 1). Although these studies confirm the functional similarity with CAT, they also reveal a number of unexpected features, particularly regarding CoA binding.

MATERIALS AND METHODS

Preparation of the Crystals. The catalytic domain (E2pCD) was prepared as a fusion protein containing residues 382–637 (i.e., the entire catalytic domain plus a few preceding N-terminal residues) of the *A. vinelandii* E2p and six residues of β-galactosidase at its N-terminus (Schulze et al., 1991). Native crystals of this fusion protein (space group $F432$, a = 224.8 Å) were grown at pH 7.0 using 16% saturated ammonium sulfate as a precipitant, employing the hanging drop method combined with the macroseeding technique (Mattevi et al., 1992b). The crystals were harvested in an artificial mother liquor containing 20% saturated ammonium sulfate, 0.02% NaN_3, and 50 mM Hepes, pH 7.0. The soaking experiments (Table I) were carried out over a period of 24 h using ligand concentrations of 10–20 mM. In order to avoid oxidation of the reactive thiols of CoA and Lip($SH)_2$, dithiothreitol (DTT) and sodium dithionite were employed.

Data Collection and Processing. For data collection, crystals were mounted in thin-walled glass capillaries flanked on both sides by two columns of soaking solution, one of them also containing 20 mM sodium dithionite. For experiments 1–5 (Table I), the diffraction data were collected on a FAST television area detector operated with a GX-21 Elliott rotating anode equipped with a graphite monochromator, using the same experimental setup as for the native crystals (Mattevi et al., 1992b). Complete data sets could be obtained from one crystal within a period of 1–2 days. The FAST data were processed by the program MADNES (Messerschmidt & Pflugrath, 1987). The intensities were then obtained by profile fitting (Kabsch, 1988).

The diffraction data of the crystal soaked in 10 mM Lip-($SH)_2$ and 10 mM dithionite, i.e., experiment 6 in Table I, were collected on the X31 beam line of the DESY synchrotron in Hamburg (Germany). Data were recorded on a Hendrix-Lentfer image plate scanner by the oscillation method. The oscillation angle was 0.5°, and the crystal-to-detector distance was set to 200 mm. The wavelength of the incident beam was 1.0 Å. The data were processed at 2.3-Å resolution using a modified version of the CCP4 (Machin et al., 1983) suite of programs. In the highest resolution shells (2.5–2.3 Å), the

[1] Abbreviations: E2p, dihydrolipoyl transacetylase (EC 2.3.1.12); E2o, dihydrolipoyl transsuccinylase (EC 2.3.1.61); E2b, dihydrolipoyl transacylase part of the branched-chain oxo acid dehydrogenase complex (EC 1.2.4.1); CAT, chloramphenicol acetyl transferase (EC 2.3.1.28); rms, root mean square; Lip($SH)_2$, dihydrolipoamide; DTT, dithiothreitol.

Table I: The Soaking Experiments

binding experiment[a]	no. unique refins	R_{merge}[b] (%)	resolution (Å)	R_{model}[c] (%)	no. waters	rms bonds[d] (Å)	rms angles[d] (deg)	rms coord[e] (Å)	⟨B⟩ protein (Å²)	⟨B⟩[f] ligands (Å²)
1. 10 mM $Lip(SH)_2$, 10 mM CoA, 100 mM DTT	13040	5.4	10.0–2.6	19.8	42	0.018	3.5	0.23	18.8	$Lip(SH)_2$, 63.6 CoA, 33.2
2. 10 mM acetyl CoA	13751	5.2	10.0–2.6	19.8	47	0.017	3.4	0.20	17.7	acetylCoA, 76.8
3. 10 mM CoA, 20 mM DTT	13641	5.4	10.0–2.6	20.3	36	0.018	3.5	0.23	17.7	CoA, 41.4 DTT, 65.3
4. 20 mM CoA, 20 mM $Na_2S_2O_4$	13596	5.2	10.0–2.6	20.0	45	0.018	3.5	0.23	16.8	CoA, 36.7
5. 15 mM $Lip(SH)_2$, 15 mM DTT	10148	5.3	10.0–3.0	18.7	30	0.018	3.4	0.23	15.4	$Lip(SH)_2$, 62.7
6. 10 mM $Lip(SH)_2$, 10 mM $Na_2S_2O_4$	21825	9.4	6.0–2.3	19.8	140	0.014	3.1	0.25	28.9	SO_2OH^-, 31.1

[a] The soaking time was 24 h for all experiments. For data collection, the crystals were mounted in the soaking mother liquor. [b] The R_{merge} is defined as $R_{merge} = \Sigma|I - \langle I\rangle|/\Sigma I$. [c] The R_{model} is defined as $R_{model} = \Sigma|F_{calcd} - F_{obsd}|/\Sigma F_{obsd}$, where F_{calcd} values are the structure factors calculated from the model. [d] The rms differences from the ideal values for the bonds and angles were calculated with XPLOR (Brünger et al., 1987). [e] The rms difference in the backbone atom positions between the complex and the native E2pCD (Mattevi et al., 1992b). [f] The average B factors of the bound ligands.

merging R factor is rather high (30%), which is most likely related to the strong radiation sensitivity of the soaked crystal. Nevertheless, all data were included in the refinement because, thanks to the high crystallographic symmetry, there are on average as many as 10 observations per independent reflection. Due to several overloaded intensities, the data below 6.0 Å

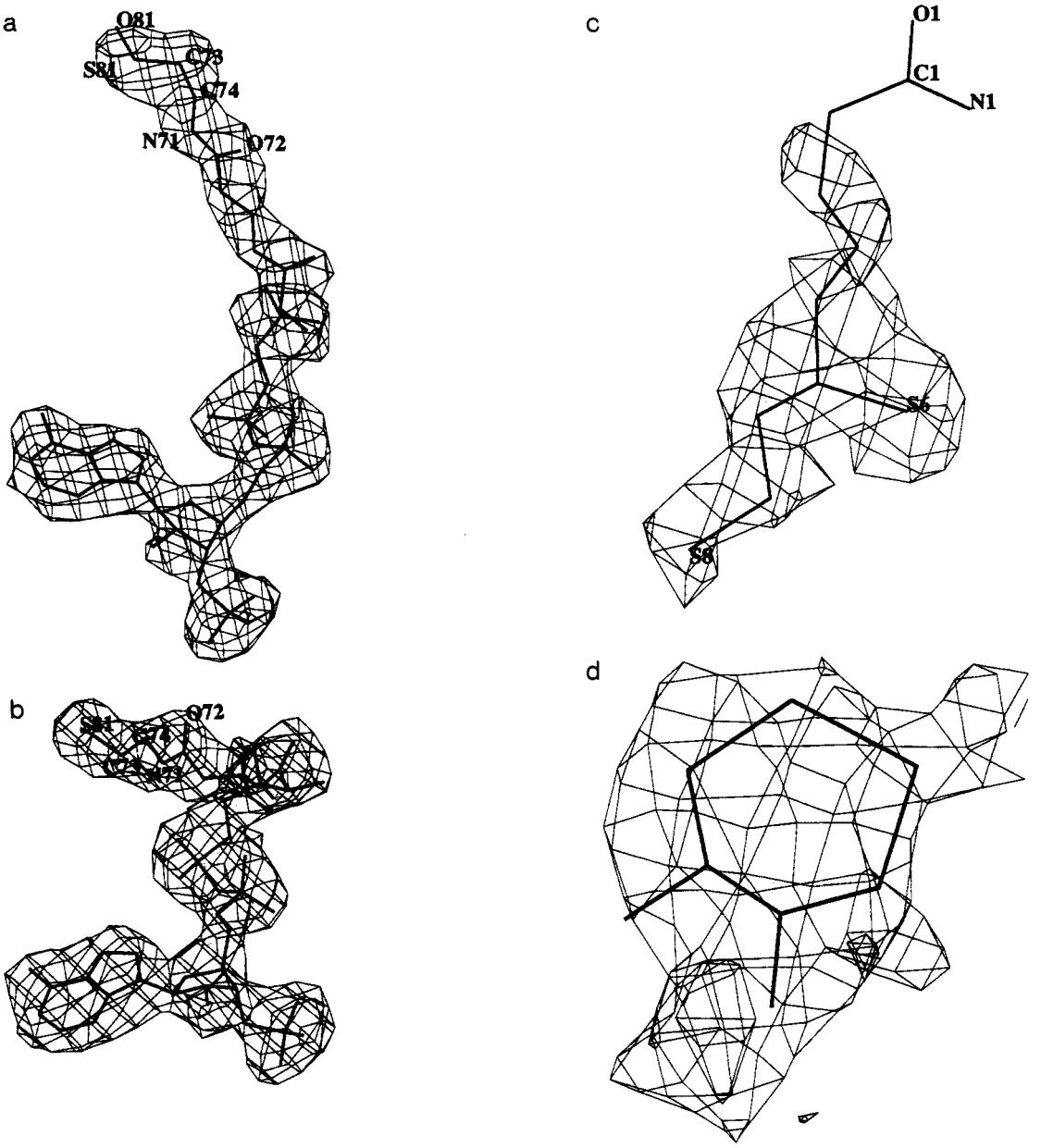

FIGURE 2: Difference $F_o - F_c$ σ_A weighted Fourier maps for the various ligands: (a) CoA in the IN conformation (soaking experiment 4 as listed in Table I); (b) CoA in the OUT conformation (soaking experiment 1); (c) $Lip(SH)_2$ (soaking experiment 1); (d) DTT (soaking experiment 3). The maps were calculated before the ligand atoms were used in the refinement and phase calculation. The contour level is 2.5σ and the resolution is 2.6 Å. In d, the poor density of DTT is most likely caused by the binding of a mixture of oxidized and reduced DTT molecules.

are largely incomplete and have not been included in the refinement.

Crystallographic Refinement. The soaking did not cause any significant change in the cell dimensions, which therefore were set to values identical to those of the native crystals. Already the initial $F_o - F_c\ \sigma_A$ weighted maps (Read, 1986) calculated with model phases revealed the ligand conformations quite clearly. These maps could be further improved by several cycles (100–200 steps) of energy minimization and *B* factor refinement, which were carried out by the program XPLOR (Brünger et al., 1987). At this stage, the various ligands were modeled (Jones, 1978) into the $2F_o - F_c$ and $F_o - F_c\ \sigma_A$ weighted maps (Figure 2) and included in the refinement. With the exception of hydrogen sulfite, the stereochemical, van der Waals, and electrostatic parameters of the bound molecules were defined according to those already present in the XPLOR library for similar chemical groups. The *R* stereoisomer of lipoamide was used (Yang & Frey, 1989). The geometrical parameters for the SO_2OH^- isomer of hydrogen sulfite were set to the values indicated by ab initio calculations (Strömberg et al., 1983).

For the refinement, all measured FAST data with resolution higher than 10 Å were used, but only data with resolution higher than 6 Å were used for the data collected with the crystal soaked in 10 mM $Lip(SH)_2$ and 10 mM dithionite (E2pCD:SO_2OH^-) for reasons described above. The final models have *R* factors ranging from 18% to 20% (Table I). As described below, substrate binding has little or no effect on the protein conformation. Therefore, although the protein electron density was carefully investigated, virtually no manual model building (Jones et al., 1991) was required. This also applies to the E2pCD:SO_2OH^- complex, whose diffraction data were collected using the strong synchrotron beam. In this case, however, the extension of the resolution from 2.6 to 2.3 Å revealed the positions of several additional water molecules, which were assigned to peaks above 3σ in the $F_o - F_c$ map and retained only if engaged in at least one H-bond with a protein or solvent atom. The atomic *B* factor refinement was tightly restrained, with a value for the rms difference between the temperature factors of covalently bound atoms of 3.0 Å^2.

RESULTS

Quality of the Models

The rms difference of the backbone atom positions between the native enzyme and the various complexes ranges from 0.20 to 0.25 Å (Table I), a value which is close to the error expected at this resolution as estimated by a σ_A plot (Read, 1986). This indicates that no significant changes in protein structure have been caused by substrate and ligand binding. This is confirmed by the fact that no peptide flipping or backbone dihedral transitions have occurred. Like in the native structure (Mattevi et al., 1992b), for all complexes the Ramachandran plots (Ramachandran et al., 1963) contain only two residues (Ala 567 and Ser 583) outside the allowed regions. The main-chain torsion angles of these two amino acids are less than 15° away from an energetically favorable ϕ,ψ combination. Moreover, deviations from ideal geometry are small for all complexes as shown in Table I. The correlation between the atomic *B* factors of the native and complex structures is in all cases about 0.70. In the E2pCD:SO_2OH^- complex, the average protein *B* factor is 28.9 Å^2, which is 10 Å^2 higher than in the other structures (Table I), possibly reflecting the strong radiation sensitivity of the crystal used for data collection. However, the high 0.70 correlation coefficient between the atomic *B* factors of the native structure and the E2pCD:SO_2OH^- complex indicates that the shift in the average value is an overall effect and is not due to local changes concerning the mobility of only parts of the protein. The relatively high *B* factors of lipoamide and DTT might reflect a lower occupancy or the presence of disorder. The atomic occupancies of the molecules were nevertheless set to 1.0 and not refined because of the limited resolution of the available data. In view of the close similarity of the complexes and the native protein, for a detailed analysis of the quality of the model we refer to Mattevi et al. (1992b), which describes the refined structure of E2pCD.

Difference Fourier Maps

The difference Fourier maps, calculated prior to the inclusion of the ligands into the model used for refinement and phase calculation, are good and unbiased indicators of the accuracy of their structures. In spite of the limited resolution, these maps (Figure 2) allow a rather clear definition of the substrate and inhibitor conformations. This is particularly evident for CoA, while in the case of lipoamide the difference Fourier map does not indicate the position of part of the aliphatic tail or the position of the carboxy amide moiety. This could indicate some disorder or incomplete occupancy related to the high *B* factor (Table I). The same considerations also apply for DTT, which was modeled in the oxidized state.

The electron density for CoA soaked together with dithionite (experiment 4 in Table I) shows an additional feature in the proximity of the reactive sulfur (Figure 2a) suggesting the oxidation of the sulfhydryl group of CoA to sulfenic acid, which is indicated by the extra oxygen, O81, in Figure 2a. Soaking with acetylCoA (experiment 2 in Table I) was unsuccessful in revealing the acetyl group position. This is most likely due to hydrolysis of the acetyl group and consequent binding of a mixture of oxidized and acetylated substrates, which make the electron density map around the reactive sulfur difficult to interpret. Apart from that, binding of acetylCoA is virtually identical to that observed in the E2pCD:CoA complex, with an rms difference of 0.42 Å for all 48 atoms of CoA. Therefore, the results of this acetylCoA soaking experiment with not be discussed further.

Location of the Binding Sites: The Active Site Channel

The substrate binding sites in E2pCD are located at the interface between two 3-fold-related subunits (Figure 3) in agreement with the conclusions by Mattevi et al. (1992b), determined by comparison of the three-dimensional structures of E2pCD and chloramphenicol acetyl transferase (CAT). The opposite entrances of a remarkable 30 Å long channel form the CoA and $Lip(SH)_2$ binding pockets, respectively (Mattevi et al., 1992a,b). The reactive sulfurs of the ligands bind in the proximity of the histidine–serine (His 610′-Ser 558) pair which is at the heart of the catalytic center, being directly involved in the transacetylase reaction (Lewendon et al., 1990). As already reported (Mattevi et al., 1992b), the E2pCD active site is one of the least mobile parts of the protein molecule. This might relate to the fact that substrate binding does not cause any large conformational change (Table I). The only significant movements are observed for Asp 508 and Asn 614′ (see Figure 8c) upon CoA binding and, to a lesser extent, for Asn 424 in the $Lip(SH)_2$ complexes.

The Two Conformations of CoA

Entirely unexpectedly, the soaking experiments revealed two different CoA binding modes (Table II). When the lipoamide binding site is unoccupied, CoA assumes an extended

FIGURE 3: Stereo diagram (Kraulis, 1991) of E2pCD trimer viewed along a direction perpendicular to the 3-fold axis. The first and second subunits are shown by a ribbon representation, while only the Cα tracing of the third one is depicted. The second monomer can be distinguished from the first one by the grey dots on the outer planes of its helices and strands. The nomenclature of secondary structure elements is the same as in Mattevi et al. (1992b). Ball-and-stick models of $Lip(SH)_2$ and CoA in the IN conformation are drawn to highlight one of the three long catalytic channels, located at the interfaces between two subunits.

Table II: Dihedrals of the Two Conformations of CoA[a]

	IN conformation of CoA (deg)		OUT conformation of CoA (deg)	
torsion angle	E2pCD:CoA[b]	E2pCD:AcCoA[c]	E2pCD:CoA:DTT	E2pCD:CoA:$Lip(SH)_2$
χ_A	121	130	142	138
ribose	2′-endo	2′-endo	2′-endo	2′-endo
ω	165	171	154	153
ξ_A	64	64	52	55
θ_A	−179	−179	−122	−129
ψ_A	52	59	162	165
ϕ_A	167	168	109	115
ϕ	−33	−44	66	59
ψ	−143	−122	−158	−164
θ	−175	−162	178	−178
χ_1	−72	−99	−51	−45
χ_2	−148	−149	−71	−77
χ_3	90	92	94	99
χ_4	176	174	−176	−174
χ_5	152	169	125	125
χ_6	171	166	−72	−78
χ_7	−178	−170	116	112
χ_8	−178	−180	−179	178
χ_9	152	80	−175	165
χ_{10}	91	62	151	160
χ_{11}[§]	−165			

[a] The torsion angles of CoA in the IN and OUT conformations. The nomenclature for the various torsion angles is defined in Figure 1. [b] The conformation of CoA observed in the soaking experiment with 20 mM CoA and 20 mM $Na_2S_2O_4$ (experiment 4 in Table I). In this complex, the reactive thiol group of the substrate undergoes a partial oxidation to sulfenic acid. [c] The CoA conformation observed in the complex obtained by soaking with 10 mM AcetylCoA (experiment 2 in Table I). As explained in the text, the acetyl group is not clearly identifiable in the electron density map.

conformation with the pantetheine arm entering its binding channel and the reactive sulfur 4.0 Å away from the Nε2 atom of the catalytic His 610′ (Figure 4a). We shall call this structure the "IN" conformation of CoA, which will be described in more detail below. Conversely, in the abortive ternary complexes where $Lip(SH)_2$ or DTT is also bound, CoA adopts a more compact structure (Figure 2b) characterized by two intramolecular H-bonds (Figure 5). In this "OUT" conformation, the reactive sulfur is located 12 Å away from the catalytic residues. Remarkably, both CoA conformations completely differ from that observed in citrate synthase. In the latter, CoA has a very compact structure with the adenine ring and peptide unit formed by C44–C43–O51–N68–C62 in contact with each other (Remington et al., 1982). The adenine is not involved in any intramolecular interaction in either the IN or OUT conformation of CoA observed in E2pCD.

While the two CoA binding modes of E2pCD are totally dissimilar beyond the pyrophosphate, the adenosine 3′-phosphate moiety is bound in a virtually identical position with an rms difference of 0.6 Å for 22 atoms (Figure 5c). This suggests that the adenosine 3′-phosphate acts as an anchor, allowing the reactive arm to adopt different conformations. This is reminiscent of a similar feature of $NAD(P)^+$ observed in lipoamide dehydrogenase (Mattevi et al., 1992c) and other members of the disulfide oxidoreductase family (Karplus & Schulz, 1989; Schiering et al., 1991): in these enzymes, the nicotinamide ring of $NAD(P)^+$, anchored by the AMP moiety, shows two different binding modes depending on the redox state of the protein, with one binding mode having the nicotinamide near the flavin ring and another mode where the adenine is more at the surface. In other words in E3, like in E2p, a substrate adopts an IN and OUT conformation with AMP as an anchor.

The IN Conformation of CoA. In the E2pCD:CoA and E2pCD:acetylCoA complexes, CoA is bound in an extended conformation spanning a distance of 15.4 Å measured from the N1A atom of the adenine ring to the reactive sulfur atom. The binding channel (Figure 4a) is formed on one side by helices H2 and H3 and on the other by β-strands βE, βG, and βI. A particularly important element for substrate binding is formed by residues 559–562 on the loop connecting βG to βH. The side chain of His 562 (Figure 4) is involved in hydrogen bonds with the initial part of the pantetheine arm (Table III) and is likely to be engaged in favorable electrostatic interactions with the pyrophosphate group. As observed in

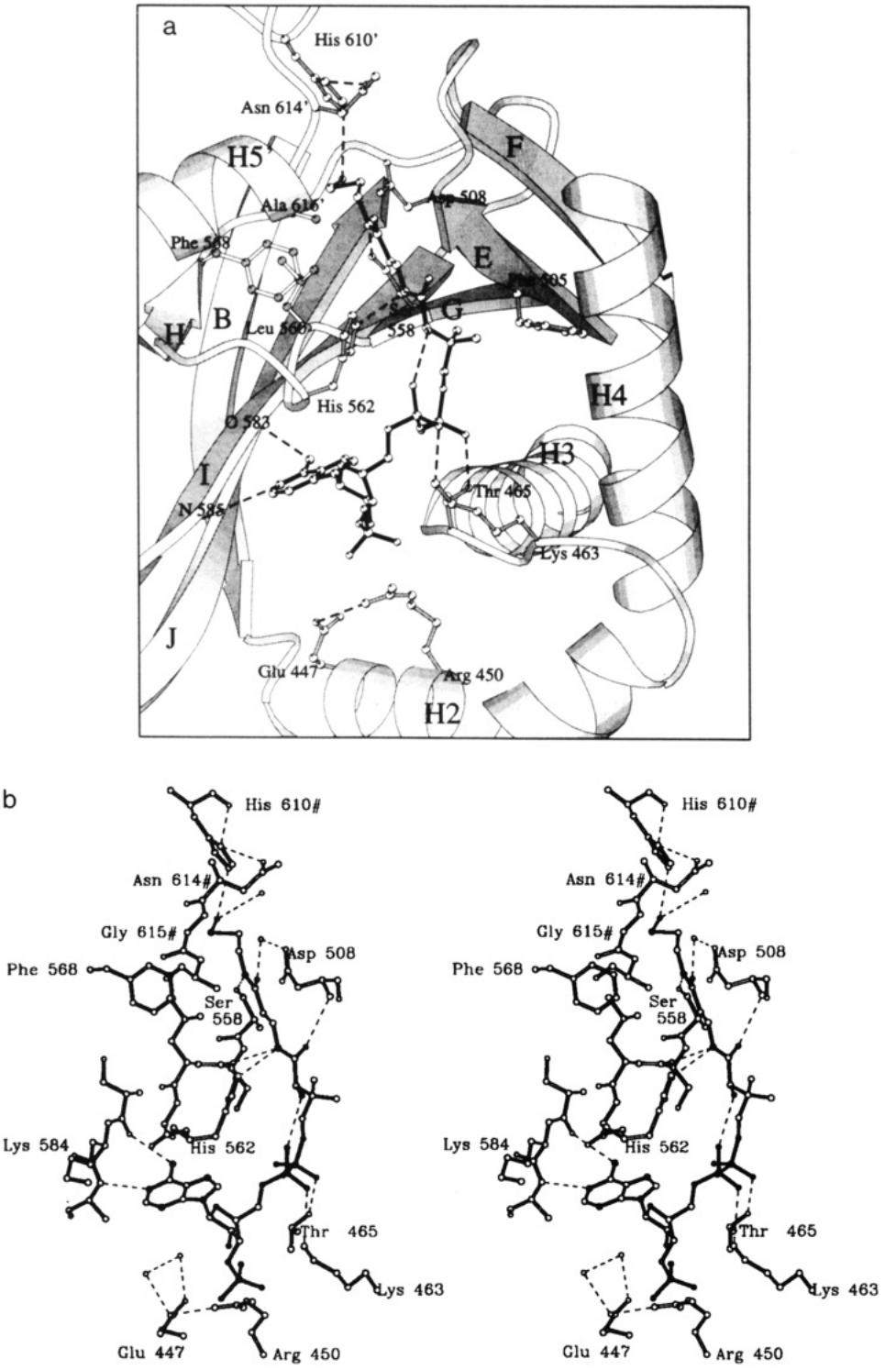

FIGURE 4: IN conformation of CoA: (a) schematic picture (Kraulis, 1991) and (b) stereo diagram (Lesk & Hardmann, 1985) of CoA bound in the productive conformation. The orientation is approximately the same as in Figure 3.

CAT (Leslie et al., 1988), this nucleotide binding site is unrelated to those found in the numerous classes of nucleotide binding proteins. We will therefore describe the binding site in some detail, referring to the complex E2pCD:CoA obtained by soaking in CoA and dithionite (Table I).

1. Adenine Ring. The adenine ring resides between strand βI and loop βG–βH. The glycosidic torsion angle is anti (Table II). There are two H-bonds with protein atoms (Table III), formed by N1A and N6A, which interact with N585 and O583, respectively, both located on strand βI (Figure 4a). The plane of the peptide between Gly 561 and His 562 is parallel to and in van der Waals contact with the adenine ring. Gly 561 is strictly conserved in all E2 sequences (Table III), possibly because any side chain at this position would collide with Ser 583 and therefore, to be accommodated, would require a structural rearrangement which would affect the adenine pocket.

2. Ribose 3'-Phosphate. The solvent-exposed ribose is in the 2'-endo conformation. The ribose does not have any direct interaction with a protein atom, and its 2'-hydroxyl group is not involved in any H-bonds. However, the 3'-phosphate is located in the neighborhood, i.e., within a distance of 4 Å, of Lys 463 and Arg 450 (Table III, Figure 4), which contributes to compensation for the negative charge of the phosphate. The side chain of Arg 450 is engaged in a salt bridge with Glu 447. This arginine residue has been the subject of mutagenesis

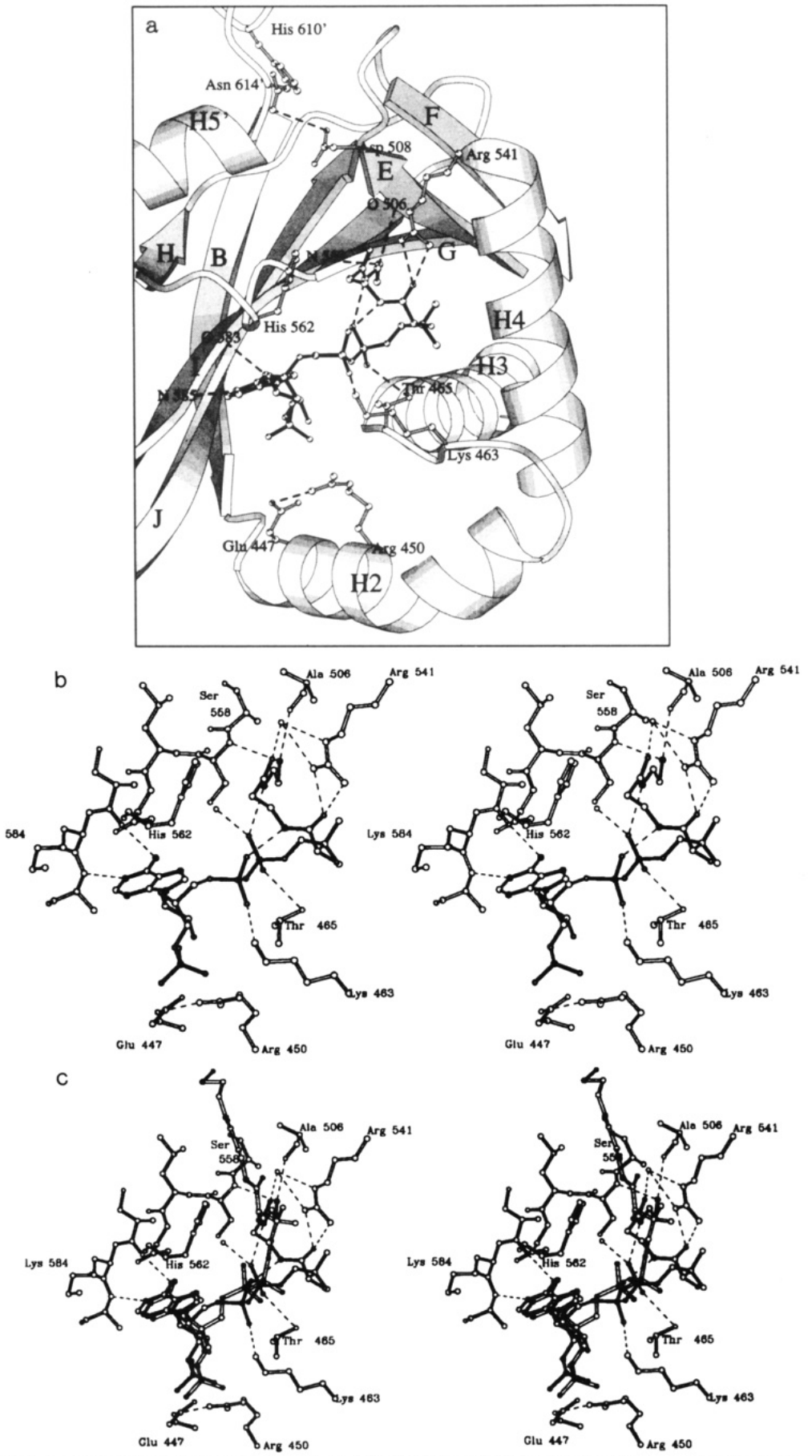

FIGURE 5: OUT conformation of CoA: (a) schematic picture (Kraulis, 1991) and (b) stereo diagram (Lesk & Hardmann, 1985) of the CoA binding site. The orientation is exactly the same as in Figure 4 and approximately the same as in Figure 3. (c) The IN (open bond representation) and OUT conformations of CoA are superimposed.

studies in the *E. coli* E2p, where it has been replaced by a glycine (Russell & Guest, 1991b). The catalytic activity of the mutated protein drops to 16% of its normal value. This observation might indicate an influence on CoA binding,

Table III: Residues within a 4.0-Å Distance from CoA in the IN Conformation

	A. vinelandii E2p contact residue[a]		H-bonds[b] atoms E2p	CoA	distance (Å)	other E2 sequences[c]
adenine ring	Val 466	side				V/L/V/I
	Gly 561	main				conserved
	His 562	main				
	Val 582	side				L/V/I/M
	Ser 583	main	O	N6αA	3.2	
	Lys 584	main + side				
	Ala 585	main + side	N	N1A	3.0	
	Leu 602	side				L/V/I/M
	Wat 310					
	Wat 312					
3′P-ribose	Arg 450	side				conserved
	Lys 463	side				K/R
	Thr 465	side				
	His 562	main + side				
	Wat 310					
pyrophosphate	Lys 463	side	Nζ	OA2	3.4	K/R
	Thr 465	side	Oγ	OP2	2.8	
pantetheine	Phe 505	side				I/V/F/M
	Ala 506	main + side				conserved
	Val 507	main				V/M
	Asp 508	main + side	N	O51	3.2	
	Arg 541	side				conserved
	Ser 558	side	Oγ	N71	3.0	conserved
	Ser 559	main	O	N68	3.1	N/S
	Leu 560	side				
	His 562	main + side	Nε2	N68	3.2	
	Phe 568	side				
	His 610′	side	Nε2	O81	3.4	
	Gly 615′	main				conserved
	Ala 616′	main				conserved
	Wat 319		OW	O69	2.7	
	Wat 321		OW	O81	3.4	
	Wat 324					
intramolecular H-bonds[d]				O52, OA1	3.2	

[a] The words main and side indicate whether the side chain or the backbone or both are within a 4.0-Å distance from CoA. Residues belonging to a 3-fold-related subunit are marked by the prime symbol. [b] The cutoff for the H-bonds is 3.4 Å. The interatomic distances (Å) refer to the CoA structure observed in E2pCD:CoA complex (soaking exp 4). The differences with respect to the conformation found in E2pCD:acetylCoA (soaking exp 2) are, however, small (rms deviation of 0.42 Å for the 48 CoA atoms). [c] On the basis of the alignment of 13 E2 sequences proposed by Russell and Guest (1991a), this column indicates whether a residue is conserved in at least 90% of the sequences or is conservatively replaced (one-letter code for the substituents). Blank spaces mean that the residue is not well conserved. [d] Intramolecular H-bonds made by the CoA atoms in the IN conformation.

although no detailed kinetic characterization was carried out.

3. Pyrophosphate. The adenine and pantetheine phosphates make direct H-bonds with the side chains of Lys 463 and Thr 465. The former residue is conserved in all E2 sequences (Russell & Guest, 1991a) while the latter is at the N-terminus of the α-helix H3 (Figure 4a), which with the NH group of Leu 467 is at distance of 4.6 Å from the OP2 oxygen of the pyrophosphate. Therefore, the N-terminus of helix H3 could have favorable electrostatic interaction with the pyrophosphate charge (Hol, 1985). In this respect, E2p differs quite significantly from CAT, where no positive charges in contact with the CoA phosphate groups are observed (Leslie et al., 1988; Day et al., 1992), although in CAT helix H3 is in a similar position as in E2pCD.

4. The Pantetheine Arm. The long arm carrying the reactive thiol binds into a crevice between strands βE and βG, adopting an extended conformation with most of its torsion angles being close to 180° (Table II). The pantetheine group is engaged in one intramolecular H-bond, bridging O52 and OA1, and seven intermolecular H-bonds (Table III). Two of the latter are made with backbone atoms, whereas five others involve a side chain or a solvent molecule. The hydrogen-bonding arrangement ensures that each hydrogen-bond donor and acceptor is forming a hydrogen bond. The pantetheine entrance into the catalytic channel causes the movement of the Asn 614′ and Asp 508 side chains (see below), the latter residue making the only water-mediated H-bond with the substrate (Figure 4b). The terminal part of the pantetheine arm is close to the N-terminus of helix H5′ from a 3-fold-related subunit (Figure 4a). Although the soaking experiment was carried out in the presence of 20 mM dithionite (Table I), the thiol group of CoA, nevertheless, seems to undergo oxidation to sulfenic acid (Figure 2). We realize that the limited resolution of data cannot rule out another cause of the extra density, but the sulfenic oxygen as modeled is hydrogen bonded to the Nε2 of His 610′ (Figure 4) and refines to a *B* factor of 38 Å^2, which is identical to that of the sulfur atom of CoA. In analogy with CAT (Leslie et al., 1988), it is likely that in the reduced substrate the reactive sulfur will directly interact with the histidine side chain.

The OUT Conformation of CoA. In both abortive ternary complexes, E2pCD:CoA:DTT and E2pCD:CoA:Lip(SH)$_2$, the adenosine 3′-phosphate of CoA binds in the same position as in the complex E2pCD:CoA, with an rms difference of 0.6 Å. However, in the ternary complexes the pantetheine arm of CoA does not enter the catalytic channel but adopts a different conformation, remaining with its reactive sulfur atom 12 Å away from His 610′ (Figure 5). The OUT conformations observed in the two independently refined ternary complexes are very similar, as indicated by an rms difference of 0.36 Å for 48 CoA atoms. In the OUT conformation CoA forms a kind of left-handed helix, with two intramolecular H-bonds involving the pyrophosphate oxygens as acceptors and the pantetheine nitrogens as donors (Table IV, Figure 5). The

Table IV: Residues within a 4.0-Å Distance from CoA in the OUT Conformation

	A. vinelandii E2p residue[a]		H-bonds[b] atoms E2p	H-bonds[b] atoms CoA	H-bonds[b] distance (Å)	other E2 sequences[c]
adenine ring	Val 466	side				F/L/V/I
	Gly 561	main				conserved
	His 562	main				
	Val 582	side				L/V/I/M
	Ser 583	main	O	N6αA	3.1	
	Lys 584	main + side				
	Ala 585	main + side	N	N1A	3.0	
	Leu 602	side				
3′P-ribose	Arg 450	side				conserved
	Lys 463	side				K/R
	His 562	main + side				
pyrophosphate	Lys 463	side	Nζ	OA2	3.0	K/R
	Thr 465	side	Oγ	OP2	3.2	
	Val 466	side				F/L/V/I
	Leu 467	main + side				
	Wat 322		OW	OP1	2.6	
pantetheine	Thr 465	side				
	Ala 506	main	O	S81	3.4	conserved
	Ala 534	side				
	Ala 537	side				
	Arg 541	side	O51	Nη1	3.3	conserved
			O51	Nη2	2.8	
	Ser 559	main + side	N	S81	3.4	
	His 562	main + side				
	Wat 322					
	Wat 338		OW	O69	3.4	
intramolecular H-bonds[d]				N68, OA1	2.7	
				N71, OP1	3.0	

[a] The words main and side indicate whether the side chain or the backbone atoms or both are within a 4.0-Å distance from CoA. Residues belonging to a 3-fold-related subunit are marked by the prime symbol. [b] The cutoff for the H-bonds is 3.4 Å. The distances refer to the CoA structure observed in the E2pCD:CoA:Lip(SH)$_2$ complex. The differences with respect to the conformation found in the ternary complex E2pCD:CoA:DTT are, however, small (rms deviation of 0.36 Å for the 48 CoA atoms). [c] On the basis of the alignment of 13 E2 sequences proposed by Russell and Guest (1991a), this column indicates whether a residue is conserved in at least 90% of the sequences or is conservatively replaced (one-letter code for the substituents). Blank spaces mean that the residue is not well conserved. [d] Intramolecular H-bonds made by the CoA atoms in the OUT conformation.

latter atoms are part of the two peptide-like units of the substrate, whose carbonyl oxygens interact directly or by a water-mediated H-bond with the Nη atoms of the guanidinium group of Arg 541. Clearly, this positively charged side chain has a favorable interaction with the dipoles of the two pantetheine peptide units. In the OUT conformation the reactive thiol group binds between strands βE and βG and is engaged in two H-bonds involving N559 and O506 (Figure 5). The electron density indicates that no oxidation of the reactive sulfur occurred in the soaking experiments, leading to the complexes E2pCD:CoA:DTT and E2pCD:CoA:Lip-(SH)$_2$ (Figure 2b).

Dihydrolipoamide Binding

The soaking experiments 1 and 5 (Table I) resulted in complexes E2pCD:Lip(SH)$_2$:CoA and E2pCD:Lip(SH)$_2$, respectively. They reveal the conformation of lipoamide bound to the side of the catalytic channel opposite to CoA. The rms difference between the conformations of Lip(SH)$_2$ in the two complexes is only 0.45 Å for the 12 substrate atoms. The presence of DTT in the soaking solution, even at high concentrations, should not have significantly affected the binding of lipoamide, since the affinity of E2pCD for DTT is at least 2 orders of magnitude lower than that for lipoamide (A. H. Westphal, and A. de Kok, personal communication).

The Lip(SH)$_2$ binding site is formed by the channel entrance which points toward the outer face of the cubic core (Mattevi et al., 1992a; Figure 3). It consists of a "floor" formed by β-strands βI, βG, βE, and βF covered by helix H1, loop βE–βF, and the segment preceding helix H5′ (Figure 6a). The numerous hydrophobic side chains, which generate the walls of the pocket and are in van der Waals contact with the substrate, are well conserved in the E2p, E2o, and E2b sequences (Table V).

Aliphatic Tail. The terminal part of the aliphatic tail of Lip(SH)$_2$, i.e., carbon C2 and the carboxyamide group (Figure 1), is poorly defined in the electron density of both the E2pCD:Lip(SH)$_2$ and E2pCD:Lip(SH)$_2$:CoA complexes. By contouring the $2F_o - F_c$ map at a low level (0.8σ), they have been tentatively modeled such that an H-bond with Asn 424 (Figure 6) is formed. The latter is the only side chain which moves with respect to the native enzyme in order to accommodate the substrate. The movement of Asn 424 is entirely accounted for by the variation of the χ_1 torsion angle from −63° in the native structure to −172° in the E2pCD:Lip(SH)$_2$ complex. The partial disorder in the tail conformation might be related to the fact that lipoate and lipoamide are equally good substrates (Yang & Frey, 1989), indicating that the carboxy amide terminal group plays only a minor role in binding.

An interesting feature emerging from the analysis of the van der Waals interactions between Lip(SH)$_2$ and E2pCD is given by the short 3.2-Å distance between C6 and the carbonyl oxygen of Ile 571 (Figure 6b). This leaves the latter as an unsatisfied hydrogen-bond acceptor in the complex. Although an erroneous interpretation of the electron density due to the medium resolution of the structure cannot be absolutely excluded, it must be emphasized that in both soaking experiments Ile 571 is well defined in the electron densities with very low *B* factors, i.e., 3 and 6 Å^2 for the oxygen in the binary and ternary complexes, respectively. Furthermore, in this conformation one H-bond between the His 434 side chain and N572 can be formed (Figure 6b). The energy penalty

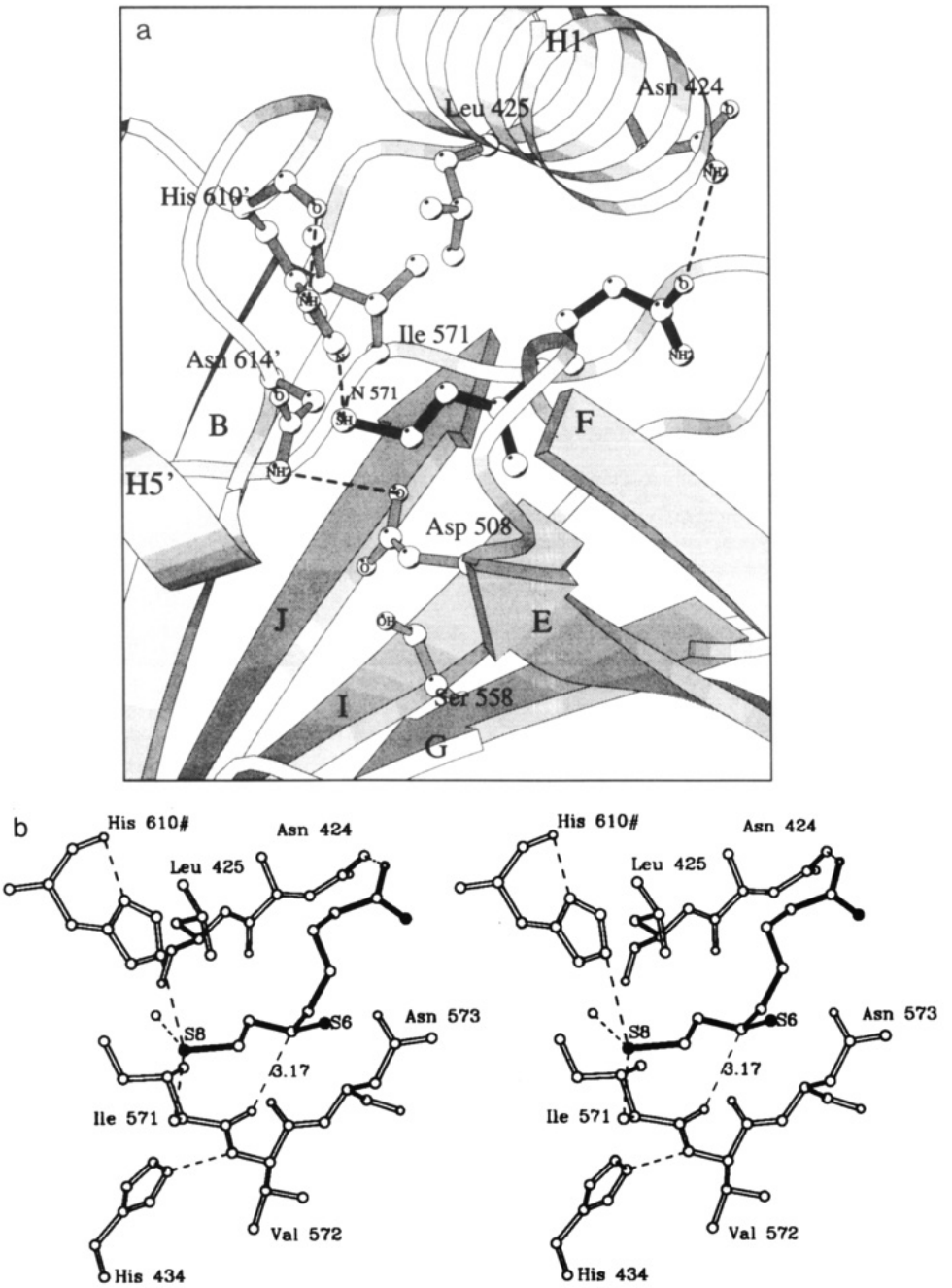

FIGURE 6: Binding of lipoamide: (a) schematic picture (Kraulis, 1991) and (b) stereo diagram (Lesk & Hardmann, 1985) of $Lip(SH)_2$ bound to E2pCD. The orientation of a is approximately the same as Figure 3. In b the short (3.2 Å) distance between the carbonyl oxygen of Ile 571 and C6 of $Lip(SH)_2$ is indicated, although it is not an H-bond.

paid for leaving an H-bond acceptor (O571) unsatisfied might find an explanation in the need to prevent inhibition by the highly hydrophobic and poorly soluble lipoamide. A completely hydrophobic and perfectly complementary channel might lead to binding that is too tight.

Reactive Sulfur. Following the studies of Yang and Frey (1986), our X-ray investigations support the specificity of E2 for the acetylation on S8 (Figure 6b). In both E2pCD:$Lip(SH)_2$ and E2pCD:$Lip(SH)_2$:CoA complexes, this sulfur is H-bonded to the Nϵ2 atom of the catalytic His 610′, in perfect analogy with CAT. Furthermore, the reactive thiol interacts with the backbone nitrogen of Ile 571 and a water molecule (Figure 6, Table V). This contrasts with the environment of S6, which remains solvent accessible, being in van der Waals contact only with the side chain of Ile 579 (Table V).

The Binding of DTT

In the initial soaking experiments, DTT was used as a reducing agent to prevent substrate oxidation. In the E2pCD:CoA:DTT complex, it was quite unexpected to see that DTT binds in the lipoamide pocket, causing CoA to be in the OUT conformation. The electron density for DTT is not very well defined (Figure 2d), but it is distinctly different from any cluster of water molecules seen in the native structure and is clearly unrelated to CoA. The ligand has been modeled in the oxidized state, but its broad density indicates that most likely a mixture of closed and open DTT molecules is bound. This relates to the fact that DTT has a high average *B* factor of 65.3 Å^2. The ligand hydroxyl groups are H-bonded to the side chain of Asn 573, whereas it is noteworthy that, like for lipoamide, there is a short contact between an aliphatic carbon of DTT and the main-chain oxygen of Ile 571. Indeed, as shown in Figure 7, the position of the bound DTT overlaps that of the dithiol moiety of lipoamide, in agreement with the fact that DTT prevents CoA from adopting the IN conformation. The position of S8 of $Lip(SH)_2$ differs by only 1.3 and 2.8 Å from the positions of the sulfur atoms of DTT. We

Table V: Residues within a 4.0-Å Distance from Dihydrolipoamide

	A. vinelandii E2p residue[a]		H-bonds[b] atoms E2p	H-bonds[b] atoms $Lip(SH)_2$	H-bonds[b] distance (Å)	other E2 sequences[c]
aliphatic tail	Asn 424	side	Nδ2	O1	3.2	N/T/R
	Leu 425	side				L/M
	Leu 513	side				conserved
	Val 515	side				V/T
	Ile 571	side				I/V
	Asn 573	main				conserved
	Ile 579	side				conserved
	His 610′	side				conserved
	Wat 326					
S6	Ile 579	side				conserved
reactive sulfur (S8)	Pro 570	side + main				
	Ile 571	main	N	S8	3.0	conserved
	His 610′	side	Nε2	S8	3.2	conserved

[a] The words main and side indicate whether the side chain or the backbone atoms or both are within a 4.0-Å distance from $Lip(SH)_2$. Residues belonging to a 3-fold-related subunit are marked by the prime symbol. [b] The cutoff for the H-bonds is 3.4 Å. The distances refer to the structure observed in E2pCD:CoA:$Lip(SH)_2$. The differences with respect to the conformation found in the E2pCD:$Lip(SH)_2$ complex are, however, small (rms deviation of 0.45 Å for 12 atoms). [c] On the basis of the alignment of 13 E3 sequences proposed by Russell and Guest (1991a), this column indicates whether a residue is conserved in at least 90% of the sequences or is conservatively replaced (one-letter code for the substituents).

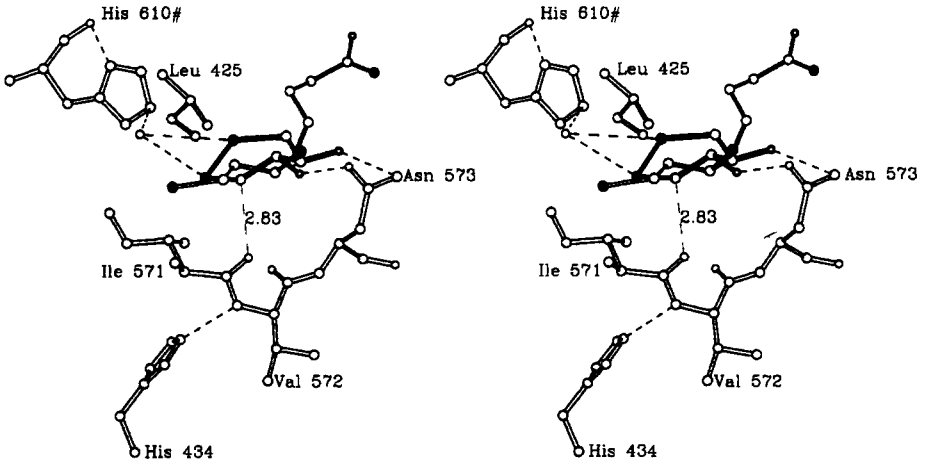

FIGURE 7: Stereo diagram of oxidized DTT (solid bond) bound to E2pCD. The short (2.9 Å) contact with the carbonyl oxygen of Ile 571 is indicated by the dashed line. The position of DTT overlaps that of lipoamide, whose structure observed in the ternary complex E2pCD:CoA:$Lip(SH)_2$ is shown by the open bond representation.

refrain from presenting a detailed analysis of the binding mode of DTT in view of its ill-defined electron density.

Negative Charge in the Active Site: SO_2OH^- Binding

After the unexpected result with DTT, we turned to $Na_2S_2O_4$ for keeping the reactive thiols reduced. In soaking experiment 6, this quite surprisingly led to the appearance of a well-defined electron density in the middle of the active site channel (Figure 8a), while no trace of $Lip(SH)_2$ could be observed. The extra density had a maximum of 4.5σ in the $2F_o - F_c$ map, and its shape strongly suggests that it is due to the product of the hydrolysis of dithionite, i.e., a hydrogen sulfite ion. The H-bond pattern indicates that the SO_2–OH^- rather than the HSO^- isomer (Strömberg et al., 1983) is bound (Figure 8a,b). The HSO^- isomer could not be modeled in a position where short contacts between the negatively charged oxygens and the carboxylate of Asp 508 could be avoided. Conversely, the protonated oxygen of the SO_2OH^- isomer (Figure 8b) is engaged in a bifurcated H-bond with the Asp 508 side chain, whereas the two unprotonated oxygens interact with the two catalytically crucial residues: Nε2 of His 610′ and Oγ of Ser 558. This H-bond scheme implies that His 610′, supposedly neutral in the native protein (see below), becomes protonated and therefore charged in the E2pCD:SO_2OH^- binary complex. In this way, the histidine can compensate for the negative charge of the bound ion, adding its effect to that of the N-terminus of helix H5′, which with the NH group of Gly 615′ is hydrogen bonded to the sulfur atom of the ligand (Figure 8b). In this context, the binary complex is particularly significant for catalysis, since during the transacetylase reaction a negatively charged covalent intermediate is likely to be formed, in analogy with CAT (Lewendon et al., 1990; Scheme I). The complex with SO_2OH^- shows that indeed the E2pCD catalytic center is suited for the stabilization of such a negative charge, located between the His 610′-Ser 558 catalytic pair.

Understanding the Role of Asn 614′

The binding of hydrogen sulfite to the catalytic center promotes the movement of the Asn 614′ side chain, which rotates about the χ_1 torsion angle from the native conformation ($\chi_1 = 50°$), in which Nδ2 is H-bonded to Asp 508, to a new position ($\chi_1 = 74°$) that allows the interaction between Oδ1 of Asn 614′ and Nδ1 of His 610′ (Figure 8b). This conformational change *cannot* be ascribed to any steric hindrance, since the asparagine side chain is not in contact, i.e., farther away than 4 Å, with the hydrogen sulfite ion. Therefore, the change in χ_1 must be considered as a response to the His 610′ protonation. The unusual conformation of the latter residue in both E2p (Mattevi et al., 1992b) and CAT

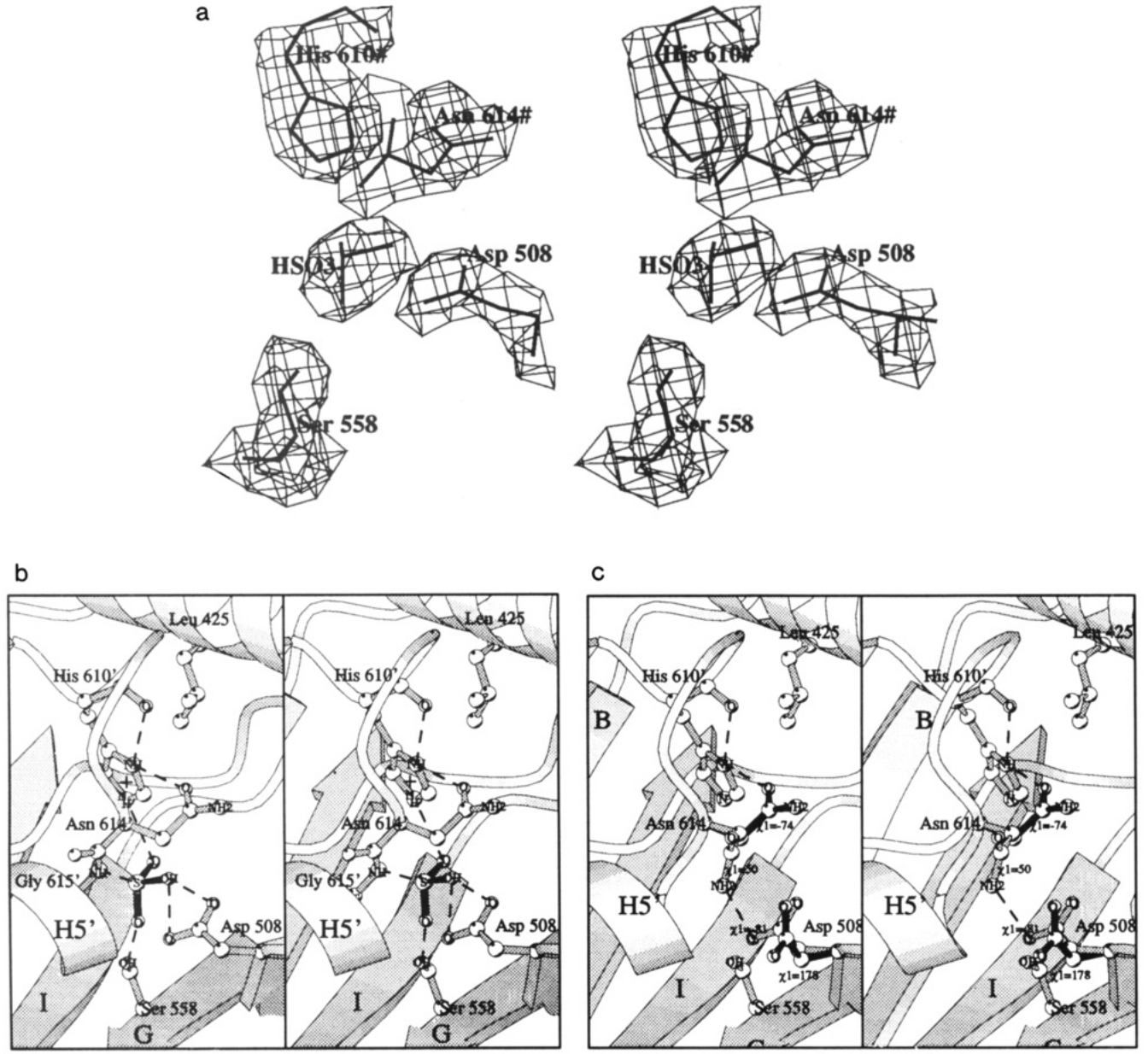

FIGURE 8: Binding of SO_2OH^- to E2pCD. (a) Final $2F_o - F_c$ σ_A weighted "omit" electron density map for the SO_2OH^- ion bound to E2pCD. Also, the electron densities of His 610′, Asn 614′, Asp 508, and Ser 558 are shown. These side chains and the atoms of the bound ion have not been included in the model used for the calculation of the map. The contour level is 1σ and the resolution is 2.3 Å. (b) Stereo "Molscript" (Kraulis, 1991) schematic drawing of SO_2OH^- bound in the catalytic center of E2pCD. The H-bond distances between the SO_2OH^- and the protein atoms are the following: O–Nϵ2 His 610′, 2.7 Å; O–Oγ Ser 558, 3.0 Å; O–Oϵ1 Asp 508, 2.6 Å; O–Oϵ2 Asp 508, 3.0 Å; S–N Gly 615′, 3.3 Å. (c) Variability in the conformations of Asn 614′ and Asp 508. In the native enzyme (gray bonds) the two side chains are hydrogen bonded to each other. Upon CoA binding, they go through a rotation about the χ_1 torsion angles (solid bond representation), moving away from each other. In the new conformation, the side-chain oxygen of Asn 614′ makes an H-bond to Nδ1 of His 610′. The Asp 614′–Asp 508 movement leaves the remaining active site residues virtually unchanged. As shown in b, in the E2pCD:SO_2OH^- complex there is a mixed situation, with Asp 508 in the native conformation and Asn 614′ rotating to interact with the protonated histidine.

Scheme I: Putative Reaction Mechanism of E2pCD Analogous to the One Proposed for CAT (Lewendon et al., 1990; only the essential His 610′ is shown for simplicity)

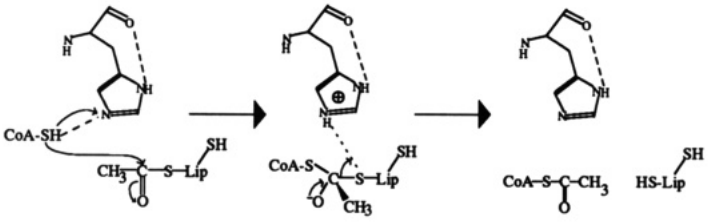

(Leslie, 1990) allows its carbonyl oxygen to be H-bonded to Nδ1 (Figure 8b), assuring the presence of the correct tautomer of the imidazole side chain (Lewendon et al., 1990). In the binary E2pCD:SO_2OH^- complex, upon the histidine protonation, Asn 614′ moves to provide an additional H-bond acceptor for Nδ1 of His 610′, in this way adding a further stabilizing interaction for the now changed imidazole ring of the side chain.

The conformational change of Asn 614′ detected in the E2pCD:SO_2OH^- complex is part of a puzzling set of

Table VI: Residues Forming the Catalytic Center in CoA Acyltransferases

A. vinelandii E2p[a]	E2p[b]	E2b	E2o
Val 435	Y/F/V	F	L
Ala 506	conserved	conserved	conserved
Val 507	conserved	M/T	conserved
Asp 508	S/A/D	D/Q	S/A
Leu 513	conserved	conserved	conserved
Ser 558	S/T	S/T	S/T
Ser 559	N/S	N/S	N
Leu 560	L/M/I	I/L	G
Phe 568	conserved	S	S
Pro 570	P/A/S	P	P
Ile 571	conserved	V	conserved
Ile 579	conserved	conserved	conserved
Tyr 608′	C/F	A/F	Y
His 610′	conserved	conserved	conserved
Ile 613′	I/V	I/V	I/V
Asn 614′	D	D	D
Gly 615′	conserved	conserved	conserved
Ala 616′	conserved	A/M	K/R

[a] The *A. vinelandii* E2pCD residues forming the catalytic centers are defined as those within a 7-Å distance from SO_2OH^-, as determined in the E2pCD:SO_2OH^- complex. [b] One-letter code indicating the substituents found in the other known E2p, E2b, and E2o sequences, following the alignment of Russel and Guest (1991a) which is based on three E2b, seven E2p, and three E2o sequences.

observations concerning not only Asn 614′ but also its neighbor Asp 508. The side chain of these two residues can adopt the different conformations, so that Asp 508 and Asn 614′ can be mutually positioned in three different ways (Figure 8c): (i) They are H-bonded to each other, as observed in the native enzyme and in the E2pCD:Lip(SH)$_2$ complex. The χ_1 torsion angles are 50° for Asn 614′ and −81° for Asp 508. (ii) In the E2pCD:CoA complex, both side chains move away from each other, the new χ_1 angles being −74° for Asn 614′ and 178° for Asp 508. The structural change of the aspartate is necessary to allow the pantetheine arm to enter its pocket and adopt the IN conformation. As a consequence, the negative charge of the Asp 508 carboxylate is removed from the active center and becomes engaged in a water-mediated H-bond with CoA (Figure 4b). Interestingly, the average *B* factors of the Asp and Asn side chains are lower in the new conformations than in the native, with a decrease from 32 to 25 Å^2 for Asp 508 and from 26 to 15 Å^2 for Asn 614′. (iii) In the E2pCD:SO_2OH^- complex, only the side chain of Asn 614′ moves (χ_1 = −74°; Figure 8b) in order to interact with the protonated His 610′. At the same time, Asp 508 remains in the native conformation, being H-bonded to the only protonated oxygen of the hydrogen sulfite SO_2OH^- isomer.

Among the known E2 sequences (Russell & Guest, 1991a), *A. vinelandii* E2p is the only one with an asparagine at position 614′, whereas all others consistently have an aspartate residue here (Table VI). Furthermore, this Asp was mutated to an Asn in both yeast (Niu et al., 1990) and *E. coli* (Russell & Guest, 1991b) proteins, causing a 16-fold and a 4-fold decrease in enzyme activity, respectively. This enforces the indication of a specific role for this side chain which, consistent with our structural observations, might modulate the properties of the essential His 610′. The reason why this function can be accomplished in the *A. vinelandii* protein by the uncharged Asn 614′ instead of an aspartate is a most intriguing question, which is currently being addressed by site-directed mutagenesis. In this context, it must be noted that in CAT, Asp 199, which is homologous to Asn 614 of E2p, is yet involved in another type of interaction. It forms a salt bridge with Arg 18 which is essential for the structural integrity of the catalytic center, as deduced from crystallographic and mutagenesis studies (Gibbs et al., 1990). Due to a deletion, Arg 18 of CAT does not have a counterpart in E2p (Mattevi et al., 1992a). Hence, the comparison with CAT does not increase our understanding of the role of Asn 614 in E2p of *A. vinelandii*.

DISCUSSION

CoA Binding. The soaking experiments presented in this study reveal that CoA has two differential binding modes. In the binary complex E2pCD:CoA, the substrate adopts an extended conformation, which allows a direct interaction with the catalytic residues. On the contrary, in the ternary complexes E2pCD:CoA:Lip(SH)$_2$ and E2pCD:CoA:DTT CoA, the substrate forms a sort of helical structure which keeps the reactive pantetheine arm outside the channel leading to the active site amino acids. The comparison (Table II, Figure 5c) of the two binding modes outlines the following points: (i) The adenosine 3′-phosphate moiety binds in virtually the same positions in the IN and OUT structures, with an rms difference of 0.6 Å for 22 atoms. The conformation of the adenine ribose group is similar to that observed in mono- and polynucleotides (Arnott & Hukins, 1969), that is, the glycosidic bond is anti and the ribose pucker is 2′-endo. (ii) In both cases, the negative charge of the pyrophosphate moiety is compensated for by the interactions with the side chains of Lys 463 and Thr 465 (Figure 5b). Moreover, in the OUT conformation, the pyrophosphate oxygens are engaged in two intramolecular H-bonds with the peptide-like units of the pantetheine arom, which can further compensate the negative charge. (iii) The conformations of the pyrophosphate group and of the pantetheine arm are quite different in the two binding modes. The torsion angles for the two conformations of CoA are listed in Table II. When the average values between the E2pCD:CoA and E2pCD:acetylCoA complexes for the IN conformation and between the E2pCD:CoA:DTT and E2pCD:CoA:Lip(SH)$_2$ complexes for the OUT conformation are compared, it appears that nine torsion angles, i.e., θ_A, ψ_A, ϕ_A, ϕ, χ_1, χ_2, χ_5, χ_6, and χ_7, differ by more than 30°. Five of these, i.e., θ_A, ϕ_A, χ_5, χ_6, and χ_7, are due to angles which are trans in the IN but not in the OUT conformation, whereas only ψ_A is trans in the OUT and not in the IN binding mode. (iv) All H-bond donors and acceptors of the pantetheine arm are engaged in hydrogen-bond interactions in both the IN and OUT conformations.

The OUT conformation of CoA is observed in the abortive E2pCD:Lip(SH)$_2$:CoA complex. If CoA were in the IN conformation, the Lip(SH)$_2$ and CoA reactive sulfurs would compete for the same H-bond acceptor (Nϵ2 His 610′) and would be at a rather short distance from each other (3.2 Å), as can be deduced from simply superimposing the structures of the E2pCD:CoA and E2pCD:Lip(SH)$_2$ complexes. The steric hindrance and the competition for the same H-bond acceptor might be the trigger for CoA to switch to the OUT conformation, where all hydrogen-bond donors and acceptors (Figure 5) are engaged in numerous H-bonds. DTT may have a similar effect since its position overlaps with that of Lip(SH)$_2$. The question can be raised why CoA should ever extend into the catalytic channel, since in the OUT conformation it can be involved in extensive interactions with the protein atoms and can form two intramolecular H-bonds between the pyrophosphate oxygens and the nitrogens of the two peptide-like units. As noted above, in the IN conformation most of the torsion angles of CoA can adopt the more favorable trans conformation by extending into the catalytic center. This observation might be an important reason supporting the fact that CoA adopts the IN instead of the OUT conformation when lipoamide or DTT does not occupy the lipoamide binding site. Furthermore, CoA must also adopt the IN conformation in the presence of acetyllipoamide in

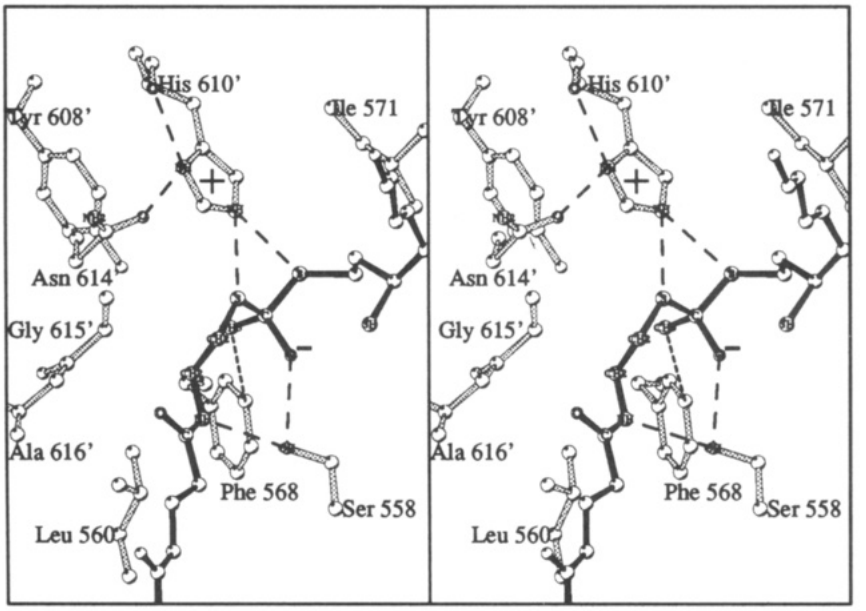

FIGURE 9: Stereo picture of the model (see text) for the covalent tetrahedral intermediate that might be formed during the transacetylase reaction in E2p, in analogy with CAT. The modeling experiment, in agreement with the analysis of the primary sequences (Table VI), suggests that the side chains at positions 560, 568, and 616′ might play a major role in the various substrate specificities among the transacylases, E2p, E2b, and E2o.

order to undergo the transacetylase reaction. The acetylated S8 atom of acetyllipoamide cannot make an H-bond with the Nε2 atom of the catalytic His 610′ which, therefore, is able to interact with the reactive thiol group of CoA. In this way, the latter can be deprotonated, leading to the formation of the putative tetrahedral intermediate occurring during the reaction (see below). Whether the observed double conformation of CoA is of any relevance to the activity of the pyruvate dehydrogenase complex remains to be investigated.

The Catalytic Mechanism. The similarity between E2pCD and CAT in their primary (Guest, 1987) and tertiary (Mattevi et al., 1992a) structures led to the prediction that the two enzymes catalyze the acetyltransferase reaction by using homologous residues with a similar mechanism. In CAT (Leslie, 1990; Lewendon et al., 1990), the reaction is initiated by His 195′ (homologous to His 610′ of E2pCD), which abstracts a proton from chloramphenicol promoting the attack of chloramphenicol on the carbonyl carbon of acetylCoA. This leads to the formation of a charged tetrahedral intermediate, which rearranges to form the products (Scheme I). In agreement with most of the mutagenesis data on E2p's from different sources (Russell & Guest, 1990, 1991b; Griffin & Chuang, 1990; A. H. Westphal, and A. de Kok, manuscript in preparation), our structural investigations generally confirm these hypotheses: (a) Hist 610′ seems to be ideally suited for acting as a base. The binary complexes with CoA and Lip-$(SH)_2$ indicate hydrogen bonds between the Nε2 of this histidine and the reactive sulfurs of both substrates. Furthermore, like in CAT, the unusual histidine conformation allows the H-bond between the carbonyl oxygen and Nδ1, ensuring the presence of the correct side-chain tautomer. (b) Although with the caveat that in all other transacylases Asn 614′ is replaced by an aspartate, this residue is likely to play a role in the modulation of the function of the general base, as discussed above. (c) The SO_2OH^- binding gives a clue about the elements which stabilize the negatively charged tetrahedral intermediate. They are the N-terminus of helix H5′ and, more directly, the hydroxyl of Ser 558, which is homologous to Ser 148 of CAT and has been proven to be essential for catalysis by site-directed mutagenesis in CAT (Lewendon et al., 1990), in *E. coli* E2p (Russell & Guest, 1991b), and *A. vinelandii* E2p (A. H. Westphal, and A. de Kok, manuscript in preparation). Its mutation to alanine reduces the catalytic efficiency of the *E. coli* enzyme to 4% of the wild-type activity.

Substrate binding causes virtually no significant structural changes in the protein molecule, suggesting that during catalysis the residues surrounding the active site retain the native conformation. By relying on this assumption and on the basis of the similarity with CAT, an idealized model for the putative covalent intermediate was built using the program O (Jones et al., 1991). For this purpose, the standard geometrical parameters for the tetrahedral carbon were used. The choice between the two stereoisomers of the tetrahedral carbon was based on the fact that only one stereoisomer allows favorable interactions between the protein atoms and both the methyl group and the charged oxygen of the intermediate. The substrates were assumed to be in the conformation observed in the E2pCD:CoA and E2pCD:Lip$(SH)_2$ complexes, and apart from the reactive sulfurs and the preceding carbons (S81–C73 in CoA and S8–C8 in Lip$(SH)_2$), they were kept fixed. In the model of the intermediate, the reactive sulfur atoms of CoA and Lip$(SH)_2$ are, respectively, 1.5 and 0.2 Å shifted with respect to the distance observed in the binary complexes. The aims of this modeling experiment were (i) to verify the feasibility of the putative charged intermediate and (ii) to obtain some clues about the structural determinants for the different specificities among the various transacylase enzymes (see below).

Remarkably, the intermediate can be easily accommodated (Figure 9). The charged oxygen makes a good hydrogen bond to Oγ of Ser 558, and the methyl group is involved in a van der Waals interaction with the side chain of Phe 568. Although the protein atoms were not moved, no bumps or bad contacts are present in this model. Furthermore, the Oγ of Ser 558 can retain the H-bond with N68 of CoA, as observed in the E2pCD:CoA complex (Figure 9). This is a most interesting hydrogen bond, because it implies that the substrate CoA itself is involved in keeping an essential hydroxyl group of the enzyme in exactly the proper position for transition-state stabilization.

Another possible hydrogen bond may occur between S6 sulfur atom of lipoamide and the charged carbonyl oxygen of the tetrahedral intermediate. The distance between the S6

atom and the oxygen is 4.1 Å. This is a rather long distance for a sulfur-to-oxygen hydrogen bond, as the usual range is between 3.2 and 3.8 Å (Gregoret et al., 1991). However, this distance is based on a model of the intermediate, and in the actual reaction mechanism this H-bond distance could be shorter, thus providing another example of substrate-assisted transition-state stabilization.

The Substrate Specificities of E2o and E2b. The significant homology of about 25–30% identity between E2p, E2o, and E2b sequences (Russell & Guest, 1991a) gives an unambiguous indication that these proteins share not only the same fold (Mattevi et al., 1992a) but also essentially the same mechanism, since the highest similarity is detected among the residues surrounding the catalytic center (Table VI). On the other hand, E2p, E2o, and E2b specifically catalyze the transfer of an acetyl, a succinyl, and a branched acyl group, respectively, and therefore deal with substrates differing substantially in volume and, in the case of E2o, also in charge. The analysis of the amino acid sequence (Table VI) shows that the residues forming the catalytic center are highly conserved, with the exception of Asp 508, Leu 560, Phe 568, Tyr 608′, and Ala 616′.

As previously described, the side chain of Asp 508 undergoes a conformational change upon CoA binding, becoming removed from the catalytic center. Therefore, it is probably not directly involved in the acetyltransferase reaction. Moreover, this residue is variable in all three families of transacylases. Tyr 608′ is well conserved, with the exception, however, of two E2b and two E2p sequences where it is replaced by alanine and cysteine, respectively. The pattern of amino acid substitutions for the remaining three residues, Phe 568, Leu 560, and Ala 616′, is suggestive that the side chains at these positions might be crucial for modulating the various specificities. Particularly, Phe 568 of E2p is replaced in all E2o and E2b sequences by a smaller serine side chain, possibly providing space required for the larger substrate. The substitution of Leu/Ile/Met 560 by a conserved glycine in E2o can be the result of a similar requirement in space. Furthermore, in the latter enzyme, the Arg/Lys residues replacing Ala 616′ of E2p could be involved in binding and might compensate for the negative charge of the succinyl carboxylate group. The importance of Phe 568, Leu 560, and Ala 616′ is supported by their location in the three-dimensional structure, since these side chains appear to be clustered and neighboring each other. Moreover, the model of the tetrahedral intermediate described in the previous section reveals that a direct van der Waals contact between the aromatic ring of Phe 568 and the methyl group of the intermediate might be present (Figure 9). This strengthens the proposal that this residue might be a key element for tuning the enzyme specificity toward acyl groups of different sizes. These clues about the determinants for the substrate specificities among the various E2 sequences provide the basis for protein engineering studies that are currently being undertaken.

ACKNOWLEDGMENT

We thank E. Schulze, A. Westphal, and A. de Kok for providing the E2pCD fusion protein and for their continuing interest in our work.

REFERENCES

Arnott, S., & Hukins, D. W. L. (1969) *Nature (London) 224*, 886–889.

Brünger, A. T., Kuriyan, J., & Karplus, M. (1987) *Science 235*, 458–461.

Day, P. J., Shaw, W. V., Gibbs, M. R., & Leslie, A. G. W. (1992) *Biochemistry 31*, 4198–4205.

Gibbs, M. R., Moody, P. C. E., & Leslie, A. G. W. (1990) *Biochemistry 29*, 11261–11265.

Gregoret, L. M., Rader, S. D., Fletterick, R. J., & Cohen, F. E. (1991) *Proteins: Struct., Funct., Genet. 9*, 99–107.

Griffin, T. A., & Chuang, D. T. (1990) *J. Biol. Chem. 265*, 13174–13180.

Guest, J. R. (1987) *FEMS Microbiol. Lett. 44*, 417–422.

Guest, J. R., Angier, S. J., & Russell, G. C. (1989) *Ann. N. Y. Acad. Sci. 573*, 76–99.

Hanemaaijer, R., Westphal, A. H., Van der Heiden, T., de Kok, A., & Veeger, C. (1988) *Eur. J. Biochem. 179*, 287–292.

Hol, W. G. J. (1985) *Prog. Biophys. Mol. Biol. 45*, 149–195.

Jones, T. A. (1978) *J. Appl. Crystallogr. 11*, 155–164.

Jones, T. A., Zou, J. Y., & Cowan, S. W. (1991) *Acta Crystallogr. A47*, 110–119.

Kabsch, W. (1988) *J. Appl. Crystallogr. 21*, 916–924.

Karplus, P. A., & Schulz, G. E. (1989) *J. Mol. Biol. 210*, 163–180.

Kraulis, P. J. (1991) *J. Appl. Crystallogr. 24*, 946–950.

Lesk, A. M., & Hardmann, K. D. (1985) *Methods Enzymol. 115*, 153–180.

Leslie, A. G. W. (1990) *J. Mol. Biol. 213*, 167–186.

Leslie, A. G. W., Moody, P. C., & Shaw, W. V. (1988) *Proc. Natl. Acad. Sci. U.S.A. 85*, 4133–4137.

Lewendon, A., Murray, I. A., Shaw, W. V., Gibbs, M. R., & Leslie, A. G. W. (1990) *Biochemistry 29*, 2075–2080.

Machin, P. A., Wonacott, A. J., & Moss, D. (1983) *Daresbury Lab. News 10*, 3–9.

Mattevi, A., Schierbeek, A. J., & Hol, W. G. J. (1991) *J. Mol. Biol. 220*, 975–994.

Mattevi, A., Obmolova, G., Schulze, E., Kalk, K. H., Westphal, A. H., de Kok, A., & Hol, W. G. J. (1992a) *Science 255*, 1544–1550.

Mattevi, A., Obmolova, G., Kalk, K. H., & Hol, W. G. J. (1992b) *J. Mol. Biol.* (in press).

Mattevi, A., Obmolova, G., Kalk, K. H., Sokatch, J., Betzel, Ch., & Hol, W. G. J. (1992c) *Proteins: Struct., Funct., Genet. 13*, 331–351.

Messerschmidt, A., & Pflugrath, J. W. J. (1987) *J. Appl. Crystallogr. 20*, 436–439.

Niu, X. D., Stoops, J. K., & Reed, L. J. (1990) *Biochemistry 29*, 8614–8619.

Oliver, R. M., & Reed, L. J. (1982) in *Electron Microscopy of Proteins* (Harris, J. R., Ed.) Vol. 2, pp 1–48, Academic Press, London.

Perham, R. N. (1991) *Biochemistry 30*, 8501–8512.

Ramachandran, G. N., Ramakrishnan, C., & Sasisekharan, V. (1963) *J. Mol. Biol. 7*, 95–99.

Read, R. J. (1986) *Acta Crystallogr. A42*, 140–149.

Reed, L. J. (1974)(*Acc. Chem. Res. 7*, 40–46.

Reed, L. J., & Hackert, M. L. (1990) *J. Biol. Chem. 265*, 8971–8974.

Remington, S., Wiegand, C., & Huber, R. (1982) *J. Mol. Biol. 158*, 111–152.

Russell, G. C., & Guest, J. R. (1990) *Biochem. J. 269*, 443–450.

Russell, G. C., & Guest, J. R. (1991a) *Biochim. Biophys. Acta 1076*, 225–232.

Russell, G. C., & Guest, J. R. (1991b) *Proc. R. Soc. London 243*, 155–160.

Schiering, N., Kabsch, W., Moore, M. J., Distefano, M. D., Walsh, C. T., & Pai, E. F. (1991) *Nature (London) 352*, 168–172.

Schulze, E., Westphal, A. H., Obmolova, G., Mattevi, A., Hol, W. G. J., & de Kok, A. (1991) *Eur. J. Biochem. 201*, 561–568.

Strömberg, A., Cropen, O., Wahlgrem, U., & Lindqvist, O. (1983) *Inorg. Chem. 22*, 1129–1133.

Yang, Y., & Frey, P. A. (1986) *Biochemistry 25*, 8173–8178.

Yang, Y., & Frey, P. A. (1989) *Arch. Biochem. Biophys. 268*, 465–471.